Astron. Astrophys. 319, 1025–1035 (1997)

ASTRONOMY
AND
ASTROPHYSICS

Collimated jet magnetospheres around rotating black holes

General relativistic force-free 2D equilibrium

Christian Fendt⋆

Lund Observatory, Box 43, S-22100 Lund, Sweden (chris@astro.lu.se)

Received 30 April 1996 / Accepted 27 August 1996

Abstract. There is common belief that superluminal jet motion from active galactic nuclei and from galactic high energy sources originates in the magnetized environment of a rotating black hole surrounded by an accretion disk.

The structure of these jet magnetospheres follows from solutions of the so called stream equation for the force-balance between axisymmetric magnetic surfaces. In this paper, two-dimensional force-free solutions of the stream equation are numerically obtained in a general relativistic context (3+1 formalism on Kerr geometry).

We apply the numerical method of finite elements. In this approach, the regularity conditions along the light surfaces are automatically satisfied. After an iterative adjustment of the poloidal current distribution and the shape of the jet boundary, we find magnetic field configurations without kinks at the outer light surface.

The solutions extend from the inner light surface of the Kerr black hole to the asymptotic regime of a cylindrically collimated jet with a finite radius. Different magnetic flux distributions along the disk surface were investigated. There is strong evidence for a hollow jet structure.

Key words: MHD – ISM: jets and outflows – galaxies: jets – black hole physics

1. Jet formation around black holes

Jet motion originating in the close environment of a rotating black hole is observationally indicated for two classes of sources concerning mass and energy output.

The first class are the active galactic nuclei (hereafter AGN). Following the standard model, AGN jet formation develops in the magnetized environment around rotating, super massive black holes with a mass of the order of $10^8 - 10^{10}\,M_\odot$ (Sanders et al. 1989, Blandford & Payne 1982, cf. Blandford et al. 1990, Kollgaard 1994). From evolutionary arguments (accretion of angular momentum) these black holes are believed to be very rapid rotators.

In some quasars and BL Lacertae objects, the jet knots are observed to follow helical trajectories on parsec-scale with a de-projected highly relativistic speed. The high jet velocity together with a small angle between the line of sight and the propagation vector involves a time shift from knot time to observer time, and thus the projected jet motion appears as *superluminal motion*. Examples are 3C 273 (Schilizzi 1992, Abrahan et al. 1994) and 3C 345 (Zensus et al. 1995).

Radio observations have also detected superluminal motion in the Galaxy. Examples are the high energy source 1915+105 (Mirabel & Rodriguez 1994) and the X-ray source GRO J1655-40 (Tingay et al. 1995). The de-projected jet speed of both sources is surprisingly similar ($0.92\,c$). This velocity may correspond to the escape velocity from a point near the black hole (Mirabel & Rodriguez 1995). However, there are not many details known about the intrinsic sources.

In both cases, the jets are detected in non-thermal radio emission, clearly indicating a magnetic character of the jet formation and propagation.

From the introductionary remarks above, it is clear that a quantitative analysis of the jet structure in these sources must take into account both magnetohydrodynamic (hereafter MHD) effects and general relativity.

In this paper we will numerically investigate the structure of a jet magnetosphere in Kerr geometry. The calculated field distributions represent *global* solutions to the *local* cross-field force-balance equation.

The first theoretical formulation of the electromagnetic force-equilibrium in Kerr space-time around fast rotating black holes was given by Blandford & Znajek (1977) and Znajek (1977). They presented the first solutions of the problem and discovered the possibility of extracting rotational energy and angular momentum from the black hole electromagnetically (the so called Blandford-Znajek process). Okamoto (1992) investigated the black hole magnetic field structure and the black hole evolution under influence of the Blandford-Znajek process. Ex-

⋆ Present address: Landessternwarte, Königstuhl, D-69117 Heidelberg, Germany (cfendt@lsw.uni-heidelberg.de)

amining the fast magnetosonic points of the wind and the accretion, he found analytical expressions for the poloidal current and the field rotation law.

With the development of the 3+1 split of Kerr space-time (Thorne & Macdonald 1982, Macdonald & Thorne 1982, Thorne et al. 1986) the understanding of the electrodynamics of rotating black holes became more transparent. For a chosen global time, the tensor description splits up in the usual fields $\boldsymbol{B}$, $\boldsymbol{E}$, current density $\boldsymbol{j}$, and charge density ρ. The formulation of the MHD equations becomes very similar to that of flat Minkowski space, which are used in pulsar electrodynamics.

Using this powerful tool, Macdonald (1984) calculated first the numerical solutions for the magnetic field force-balance around rotating black holes. Three models (magnetic field distribution roughly radial, uniform, or paraboidal) of differentially rotating magnetospheres were investigated, however, the integration region was limited to $\lesssim 10$ horizon radii.

Camenzind (1986, 1987) formulated a fully relativistic description of hydromagnetic flows, basically applicable to any field topology. The so-called wind equation considers the stationary force-balance of the plasma motion along the magnetic field. The (flat space) transfield equation was solved by using the method of finite elements.

Haehnelt (1990) extended this procedure for Kerr space-time in the 3+1 description. The solutions explicitly show the interrelation between the poloidal current strength and the collimation of the flux surfaces. They were calculated on separate integration domains inside and outside the light cylinder (see Camenzind 1990). However, there was a mismatch between the inner and outer solution at the light cylinder, which is a singular surface of the relativistic transfield equation. This matching problem is well known from in the literature of pulsar magnetospheres (Michel 1991).

So far, no global magnetic field solutions could yet be found originating in the accretion disk close to the rotating black hole and, passing through the outer light surface, eventually reaching the asymptotic regime of a collimated jet.

The matching problem of relativistic force-free magnetospheres was investigated in the context of stellar jets (Fendt 1994, Fendt et al. 1995). It then became clear that a mismatch at the light cylinder could be removed by a proper adjustment of the current distribution and the outer boundary condition, which could be interpreted as an adjustment of the "magnetic pressure equilibrium" between the regions inside and outside the light cylinder.

In this paper, we like to extend the results from Fendt et al. (1995) to the general relativistic context. The solutions presented here are *global* solutions for the stationary black hole force-free electrodynamics in the sense that they smoothly pass the singular surface of the outer light surface. The field lines originate near the inner light surface close to a rotating black hole and collimate to an asymptotic jet of finite radius of several (asymptotic) light cylinder radii.

The structure of this paper is as follows. In Sect. 2, basic equations of the theory of relativistic magnetospheres in the context of Kerr metric are reviewed. In Sect. 3, the model underlying the numerical calculations is discussed. We present our numerical results in Sect. 4 and discuss solutions with different topologies and jet parameters.

2. MHD description of black hole magnetospheres

The basic equations describing a magnetohydrodynamic (MHD) configuration under the assumptions of axisymmetric, stationary and ideal MHD in the context of Kerr metric were first derived by Blandford & Znajek (1977) and Znajek (1977). In this paper, we apply the MHD formulation in the 3+1 formalism introduced by Thorne & Macdonald (1982), Macdonald & Thorne (1982), or Thorne et al. (1986) (hereafter TPM). In the notation, we follow TPM and Okamoto (1992).

2.1. Space-time around rotating black holes

In the 3+1 split the space-time around rotating black holes with a mass M and angular momentum per unit mass, $a = J/Mc$ is described using Boyer-Lindquist coordinates with the line element

$$ds^2 = \alpha^2 c^2 dt^2 - \tilde{\omega}^2 \, (d\phi - \omega dt)^2 - (\rho^2/\Delta) \, dr^2 - \rho^2 \, d\theta^2 \, . \quad (1)$$

t denotes a global time in which the system is stationary, ϕ is the angle around the axis of symmetry, and r, θ are similar to their flat space counterpart spherical coordinates. The parameters of the metric tensor are defined as usual,

$$\begin{aligned} \rho^2 &\equiv r^2 + a^2 \cos^2\theta & \Delta &\equiv r^2 - 2\,G\,M\,r/c^2 + a^2 \\ \Sigma^2 &\equiv (r^2 + a^2)^2 - a^2 \Delta \sin^2\theta & \tilde{\omega} &\equiv (\Sigma/\rho) \sin\theta \\ \omega &\equiv 2\,a\,G\,M\,r/c\,\Sigma^2 & \alpha &\equiv \rho\sqrt{\Delta}/\Sigma \end{aligned}$$

ω is the angular velocity of the differentially rotating space, or the angular velocity of an observer moving with zero angular momentum (ZAMO), $\omega = (d\phi/dt)_{\rm ZAMO}$, respectively. α is the red shift function, or lapse function, describing the lapse of the proper time τ in the ZAMO system to the global time t, $\alpha = (d\tau/dt)_{\rm ZAMO}$.

The electromagnetic field $\boldsymbol{B}, \boldsymbol{E}$, the current density $\boldsymbol{j}$, and the electric charge density $\rho_{\rm c}$ are measured by the ZAMOs according to the local flat Minkowski space. These local experiments then have to be put together by a global observer for a certain global time using the lapse and shift function for the transformation from the local to the global frame. In spite of this transformation, Maxwell's equations in the 3+1 split look very similar to those in Minkowski space. There is just an additional source term from the differential rotation of space (see below).

2.2. The cross–field force–balance

The magnetospheric structure follows from the force-balance across the flux surfaces. The projection of the equation of motion perpendicular to the field lines provides the stream equation. Here, in the force-free case, only Lorentz forces (perpendicular to the flux surfaces) are considered.

Under the assumption of axisymmetry a magnetic flux function (or stream function) can be defined measuring the magnetic flux through a loop of the Killing vector $\boldsymbol{m} = \tilde{\omega}^2 \nabla\phi$,

$$\Psi(r,\theta) = \frac{1}{2\pi}\int \boldsymbol{B}_{\rm P}\cdot d\boldsymbol{A}\,, \qquad \boldsymbol{B}_{\rm P} = \frac{1}{\tilde{\omega}^2}\nabla\Psi\wedge\boldsymbol{m}. \tag{2}$$

Equivalently, the poloidal current is defined by integration of the poloidal current density through the same loop

$$I = -\int \alpha \boldsymbol{j}_{\rm P}\cdot d\boldsymbol{A} = -\frac{c}{2}\alpha\tilde{\omega}B_{\rm T}\,. \tag{3}$$

The indices P and T denote the poloidal and toroidal components of a vector. The force-free assumption,

$$\rho_{\rm c}\boldsymbol{E} + \frac{1}{c}\boldsymbol{j}\wedge\boldsymbol{B} = 0\,, \tag{4}$$

implies that the poloidal current flows parallel to the poloidal magnetic field $\boldsymbol{B}_{\rm P} \parallel \boldsymbol{j}_{\rm P}$. Thus, $I = I(\Psi)$.

With the assumption of a degenerated magnetosphere, i.e.

$$|B^2 - E^2| >> |\boldsymbol{E}\cdot\boldsymbol{B}| \simeq 0 \tag{5}$$

an angular velocity of field lines can be derived from the derivative of the time component of the vector potential

$$\Omega_{\rm F} = \Omega_{\rm F}(\Psi) = -c(dA_0/d\Psi) \tag{6}$$

With the additional assumption of stationarity, Ampère's law can be expressed as

$$\nabla\wedge\alpha\boldsymbol{B} = \frac{4\pi}{c}\alpha\boldsymbol{j} - \frac{1}{c}(\boldsymbol{E}\cdot\nabla\omega)\boldsymbol{m}\,, \tag{7}$$

(TPM). The differential rotation of space provides an additional source term with the dimension of a current density. The toroidal current density follows from a projection of Eq. (4), the equation of motion in the force-free limit, perpendicular to Ψ,

$$\begin{aligned}\frac{4\pi}{c}\alpha\, j_{\rm T} = &-\frac{\alpha\,(\Omega_{\rm F}-\omega)}{c\,\tilde{\omega}}\nabla\Psi\cdot\nabla\left(\frac{\tilde{\omega}^2(\Omega_{\rm F}-\omega)}{\alpha^2\,c}\right)\\ &-\left(\frac{\tilde{\omega}}{\tilde{\omega}_{\rm L}}\right)^2\tilde{\omega}\nabla\cdot\left(\frac{\alpha}{\tilde{\omega}^2}\nabla\Psi\right)\\ &+\frac{1}{\alpha\tilde{\omega}}\frac{4}{c^2}\,I\,I'\,.\end{aligned} \tag{8}$$

The toroidal component of Ampère's law (7) eventually leads to the stream equation, a non linear partial differential equation of second order for the flux function Ψ,

$$\tilde{\omega}\nabla\cdot\left(\alpha\,\frac{D}{\tilde{\omega}^2}\nabla\Psi\right) = \tilde{\omega}\,\frac{\omega-\Omega_{\rm F}}{\alpha c^2}\Omega_{\rm F}'\,|\nabla\Psi|^2 - \frac{1}{\alpha\tilde{\omega}}\frac{4}{c^2}\,I\,I'\,. \tag{9}$$

Here,

$$D = 1 - \left(\frac{\tilde{\omega}}{\tilde{\omega}_{\rm L}}\right)^2\,, \tag{10}$$

and $\tilde{\omega}_{\rm L}$ denotes the positions of the two light surfaces,

$$\tilde{\omega}_{\rm L}^2 = \left(\pm\frac{\alpha\,c}{\Omega_{\rm F}-\omega}\right)^2\,. \tag{11}$$

The $'$ indicates the derivative $d/d\Psi$. The + sign holds for the outer light surface with $\Omega_{\rm F} > \omega$, while the $-$ sign stands for the inner light surface, where $\Omega_{\rm F} < \omega$. Throughout this paper we will assume a constant angular velocity of the field lines, $\Omega_{\rm F}(\Psi)$ =const. This assumption will be discussed below (Sect. 3.5).

The stream equation was first derived by Blandford & Znajek (1977) and further evaluated in the 3+1 formalism by TPM. A general version of the stream equation including inertial terms and entropy was obtained by Beskin & Pariev (1993).

In the special relativistic limit, $\alpha \to 1$, $\omega \to 0$, and the stream eq. (9) becomes identical to the pulsar equation (Scharlemann & Wagoner 1973).

2.3. Normalization

For large r, $\omega \to 0$ and the metric reduces to Minkowski. We define an asymptotic light cylinder, $R_{\rm L} \equiv c/\Omega_{\rm F}$ (here and in the following (R, Z) denote the cylindrical coordinates). Using the normalization

$$\begin{aligned} r &\Leftrightarrow R_{\rm L}\,r,\\ \tilde{\omega} &\Leftrightarrow R_{\rm L}\,\tilde{\omega},\\ \nabla &\Leftrightarrow (1/R_{\rm L})\,\nabla\,,\\ \Psi &\Leftrightarrow \Psi_{\rm max}\,\Psi\,,\text{ and}\\ I &\Leftrightarrow I_{\rm max}\,I\,,\end{aligned}$$

the stream equation can be written dimensionless

$$\tilde{\omega}\nabla\cdot\left(\alpha\,\frac{D}{\tilde{\omega}^2}\nabla\Psi\right) = -g_{\rm I}\frac{1}{\alpha\tilde{\omega}}\;I\,I'\,. \tag{12}$$

The coupling constant $g_{\rm I}$ measures the strength of the (poloidal current) source term,

$$g_{\rm I} = \frac{4I_{\rm max}^2R_{\rm L}^2}{c^2\Psi_{\rm max}^2} = 4\,(\frac{I_{\rm max}}{10^{18}{\rm A}})^2(\frac{R_{\rm L}}{10^{16}{\rm cm}})^2(\frac{\Psi_{\rm max}}{10^{33}{\rm Gcm}^2})^{-2} \tag{13}$$

(A similar normalization for the $\Omega_{\rm F}$ term in Eq. (9) would reveal a coupling constant $g_\Omega = 1$.)

Two typical length scales enter the problem. (1) The scale of the horizon radius $r_{\rm H}$ determines the influence of gravitation on the metric. (2) The asymptotic light cylinder $R_{\rm L}$ describes the influence of rotational effects on the electrodynamics. The interrelation between these two scaling parameters follows from the definition of the rotation law for the field, $\Omega_{\rm F}(\Psi)$, in terms of the rotation of the black hole, $\Omega_{\rm H}$.

2.4. The regularity condition

At the light surfaces, the stream equation becomes singular and reduces to a non-linear, partial differential equation of first order,

$$\nabla D\cdot\nabla\Psi = -g_{\rm I}\frac{1}{\alpha^2}I\,I'\,. \tag{14}$$

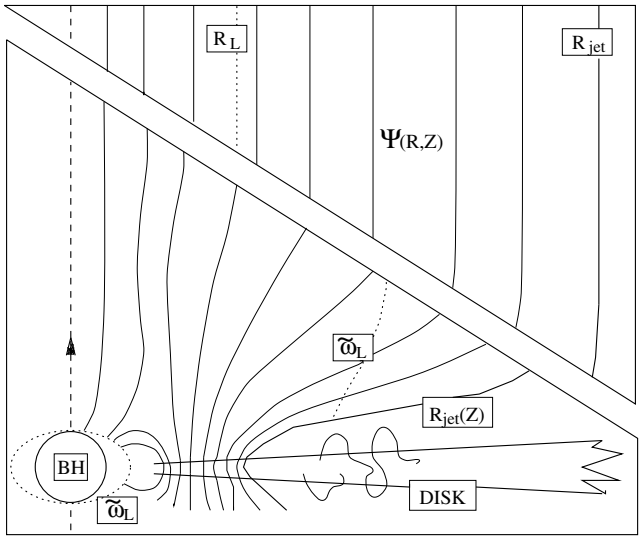

Fig. 1. Applied model topology for the jet formation around rotating black holes. The sketch shows the asymptotic region in the upper part and the inner region around the black hole (BH) in the lower part. The two regions are drawn in different scales.

This regularity condition for Ψ is equivalent to an inhomogeneous Neumann-type boundary condition on the poloidal magnetic field component parallel to the surface $D = 0$ (the light surface),

$$\frac{\partial \Psi}{\partial n} = g_{\rm I}\,\frac{1}{|\nabla D|}\,\frac{1}{\alpha^2}\,I\,I'\,, \quad \boldsymbol{n} = -\frac{\nabla D}{|\nabla D|}\,, \tag{15}$$

where $\boldsymbol{n}$ denotes the unit vector normal to the light surface.

Note that the regularity condition depends on the *strength* of the poloidal current as well as the current *distribution*. This has far reaching consequences for the global field topology. For the special relativistic case, we have shown that the shape of the jet boundary is determined by the regularity requirement (Fendt 1994, Fendt et al. 1995). As it will discussed below, the same applies in the general relativistic case.

3. The model assumptions

We now describe the model assumptions underlying the numerical calculations. The model topology basically follows the standard model for AGN (cf. Blandford 1990).

There is not very much known about the central sources of galactic superluminal jets. Since observationally the jet phenomenon of AGN and of young stellar objects as well is always connected to the signatures of an accretion disk, we assume a similar disk-jet scenario for the jet formation in *galactic* superluminal jet sources.

In the following, we discuss the three main components of the applied model - a central black hole, a surrounding accretion disk, and the asymptotic jet. A schematic overview of the model is shown in Fig. 1.

3.1. The central black hole

In the standard model for AGN the driving engine responsible for the activity is a rotating super massive black hole with a mass of about $10^8 - 10^{10}\mathrm{M}_\odot$ (Sanders et al 1989).

In the case of galactic superluminal sources, there is evidence that the central object is a black hole as well (Mirabel & Rodriguez 1995).

For the calculation of the field structure from the force-free stream equation, gravitational effects of the collapsed object play a non-obvious role. They appear in the stream equation in the description of the gravitogeometric background and in the two light surfaces.

The differential rotation of the space around Kerr black holes leads to the formation of two light surfaces (hereafter LS). Here, the rotational velocity of the field lines relative to the ZAMO equals the speed of light (see Blandford & Znajek 1977). This could be understood from the following. The concept of field lines implies the rigid rotation of each field line. Far from the hole, where ω is small, the outer LS describes the point where the field line velocity equals the speed of light seen from a static observer in the non-rotating space. Close to the hole, the space and the co-moving ZAMO is forced to (differentially) rotate. Since the field line is rigidly rotating, at a certain position (the inner LS) it will reach the speed of light in opposite direction seen from a ZAMO. Here, $\omega > \Omega_{\rm F}$, and the 'field velocity' equals $-c$.

In terms of the global jet solution, the inner LS is very close to the horizon. With the numerical method applied, there is no fundamental hindrance for a solution between the inner LS and the horizon. However, since our main interest is the jet solution, we take the inner LS as inner boundary for the integration region. The black hole horizon itself remains hidden behind the inner LS.

The Schwarzschild radius $R_{\rm S} = 2M$ defines the typical length scale for general relativistic effects,

$$R_{\rm S} = \begin{cases} 1.5\,10^6\ \left(M/5\,\mathrm{M}_\odot\right)\,\mathrm{cm} \\ 3.0\,10^{15}\ \left(M/10^{10}\,\mathrm{M}_\odot\right)\,\mathrm{cm}\,. \end{cases}$$

For rotating black holes the event horizon is changed to $r_{\rm H} = M + (M^2 - a^2)^{1/2}$. The angular velocity of the hole in terms of the Kerr parameter a and mass M is

$$\Omega_{\rm H} = \lim_{r \to r_{\rm H}} \omega = \frac{a}{2\,M}\,\frac{1}{r_{\rm H}}\,. \tag{16}$$

Here, we choose $a = 0.8$.

Mirabel & Rodriguez (1995) mentioned that the deprojected jet speed of $0.9\,c$ for the galactic superluminal jets could be related to the escape velocity from a region close to a black hole. Further, in contrast to other mildly relativistic jets ($\sim 0.3\,c$) this is indicating both a black hole as central source and, also, that the jet origin is very close to the hole at a distance of several horizon radii (Mirabel & Rodriguez 1995).

3.2. The accretion disk

An accretion disk surrounding the central black hole seems to be the essential component concerning magnetic jet formation. It is considered to be responsible for the following necessary ingredients for jet formation, propagation, and collimation.

- *Generation of magnetic field*. In contrast to pulsar or protostellar jets the magnetic field of jets from black holes, the magnetic field cannot be supplied by the central object but has to be supplied by the surrounding accretion disk.
  Khanna & Camenzind (1994, 1996a) were first to formulate the axisymmetric dynamo equations in Kerr space time. They indicated the possibility of an $\omega\Omega$ dynamo, since differential rotation of space ω provides a new source term for the dynamo action. This general relativistic dynamo effect might work very close to the black hole, at distances of about several horizon radii (Khanna & Camenzind 1996a,1996b; Brandenburg 1996).
  In our model we assume that the jet is formed by a *finite* flux distribution of the disk. The maximum flux originates from the disk at radii less than the LS radius, and $\Psi_{\rm max} \simeq 10^{33}\,{\rm G\,cm^2}$.
- *Mass injection into the jet*. The accretion disk supplies the mass for injection into the jet, since there is no mass outflow possible from the black hole itself.
  Certain disk parameters like accretion rate, magnetization and others determine the mass accretion process together with the mass ejection rate (Ferreira & Pelletier 1995). In this paper, we assume that the mass flow is not charge separated and that the plasma is highly conductive in order to justify the assumption of degeneracy (5). Further, the mass flow has to be weak enough (or highly magnetized) in order to assume a force-free source term of the stream equation.
- *The current system*. Differential rotation of the disk is responsible for the poloidal current system in the jet magnetosphere. These currents extract angular momentum from the disk and eventually allow for mass accretion into the central object.
  The poloidal current correspond to toroidal magnetic fields and its hoop stress may be responsible for a collimation of the jet.

The accretion disk physics would further determine the rotation law of the jet magnetic field, $\Omega_{\rm F}(\Psi)$ (see Sect. 3.5).

The disk evolution is definitely influenced by the evolution of the jet and vice versa (cf. Ferreira & Pelletier 1995). However, since this global problem is literally unresolved, in this paper we take into account the accretion disk only as source for the magnetic flux, i.e. as a boundary condition for the flux function Ψ.

3.3. The asymptotic jet

We assume that the asymptotic jet is collimated to a cylindrical shape. This is in agreement with VLBI observations of the knot motion in e.g. 3C 345 (Zensus et al. 1995), and also with kinematic models explaining the short period optical variations by a geometrical lighthouse effect (Camenzind & Krockenberger 1992).

In the case of the parsec-scale jet in the quasar 3C 345, the best model fits give a very small intrinsic opening angle of $\simeq 0.5^\circ$ (Zensus et al. 1995). The innermost region of the jet is not resolved observationally. In the radio VLBI measurements mentioned above, the angular beam resolution is $\sim$ 0.3 mas corresponding to $\sim$ 1 pc. This is comparable to $1000\,R_{\rm S}\,(M/10^{10}\,{\rm M}_\odot)$.

The lighthouse model of Camenzind & Krockenberger (1992) reveals a jet radius of $10\,R_{\rm L}$ for both 3C 273 and BL Lacertae objects under the assumption that the field rotates with the angular speed of the marginally stable orbit. Further, the black hole parameters were assumed to be $a = 0.9$ ($a = 0.8$) and $M = 7\,10^9\,{\rm M}_\odot$ ($M = 5\,10^7\,{\rm M}_\odot$) for 3C 273 (BL Lacertae objects). The degree of jet collimation is very high and initial opening angles of 0.1° (0.05°) are found.

In the asymptotic regime, the metric simplifies to that of flat Minkowski space. Here, the special relativistic, one-dimensional jet equilibrium of Appl & Camenzind (1993) can be applied. They were first to find a non-linear analytical solution for a cylindrically collimated, asymptotic flux distribution,

$$\Psi(x) = \frac{1}{b} \ln\left(1 + \left(\frac{x}{d}\right)^2\right) , \tag{17}$$

where $x = R/R_{\rm L}$ is defined as the cylindrical radius normalized by the asymptotic light cylinder radius. The flux distribution (17) corresponds to a core-envelope structure with core radius d. The poloidal current is concentrated within the jet core (see below). With Eq. (17) the asymptotic jet radius is defined by $\Psi(x_{\rm jet}) = 1$.

Using the method of finite elements for a numerical solution implies that we solve the *boundary* value problem. It is hence suitable to prescribe the *asymptotic* jet boundary $x_{\rm jet}$ and adjust later for the current profile parameter b (see Fendt et al. 1995 for details). This adjustment is the essential procedure in order to satisfy the regularity condition at the light surface.

In conclusion, the poloidal current distribution and the strength of the current are determined by the asymptotic jet. We choose the asymptotic jet radius in terms of asymptotic LC radii $R_{\rm jet} \simeq 3R_{\rm L}$ and $R_{\rm L} = 10\,M$.

3.4. The current distribution

The poloidal current distribution may be considered as a free function for the force-free stream function (although it is constrained by the regularity condition). In particular, since $I = I(\Psi)$ in the 3+1 description too, it is possible to apply the same current distribution for the region near the black hole as for the asymptotic, special relativistic region.

Here, we choose the analytical, non-linear solution for special relativistic (asymptotically cylindrical) pinches given by Appl & Camenzind (1993),

$$I(\Psi) = \frac{1 - e^{-b\Psi}}{1 - e^{-b}} . \tag{18}$$

The parameter b describes the shape of the current profile. Together with the flux distribution (17) this current distribution simultaneously satisfies the asymptotic transfield equation (Appl & Camenzind 1993). The current flow is concentrated within the core radius d (see Eq. (17)). The strength of the current, $g_{\rm I}$, and the shape of the profile ($b \ll 1$ diffuse pinch, $b \gg 1$ sharp pinch) control the magnetic structure and the kinematics of the jet. In particular, they determine the asymptotic jet radius and velocities.

As discussed above, in our approach we choose the jet radius as parameter and adjust the parameters $g_{\rm I}$ and b in such a way that we obtain smooth solutions across the LS with an asymptotic jet radius of a few LC radii.

Eq. (18) represents a monotonous current distribution with no return current within the jet. A closure of the poloidal current flow would be achieved via the jet hot spots terminating the jet and the interstellar/intergalactic medium. In this picture the current is generated in the disk, flows along the jet to the hot spots, and returns back to the accretion disk in the surrounding medium outside of the jet. A return current within the jet might be a more realistic concept. However, serious difficulties for a two dimensional solution are involved with such a current distribution. These are e.g. a proper satisfaction of the regularity condition, as well as the need for a proper boundary condition for the asymptotic jet. We will address this topic to our future work. The solutions presented in this paper may be interpreted as the inner part of such a return current jet.

3.5. The rotation law

As was the case with the current distribution, the rotation law for the flux surfaces is a free function of the force-free stream equation.

In general, this rotation law follows from a detailed examination of the accretion process and the dynamo action in the disk. This is far beyond the scope of this paper and the complex physics of magnetized accretion disks is not yet fully understood. Although there are several models available for the different physical processes involved, such as (magnetic) viscosity, convection, advection, diffusion, kinematics, dynamo action, or relativistic effects, for a combined treatment of all the effects the problem is far from being resolved (not to mention that the jet itself provides an important boundary condition for the disk dynamo).

Having such a solution available, the calculated rotation law, $\Omega(r)$, and flux generation, $\Psi(r)$, would determine the rotation of the magnetic field $\Omega_{\rm F}(\Psi) = \Omega(r(\Psi))$.

As an example we discuss an approximate steady state solution for the flux distribution of a thin accretion disk around a black hole, $\Psi(r) \sim \exp(-k^2 \int_r^{r_{\rm out}} D(\tilde{r}) d\tilde{r})$, where $D(r)$ is the diffusion parameter of the diffusion equation (Khanna & Camenzind 1992). For radii larger than the marginally stable orbit, $D(r) \sim r^{-2}$, and the integration gives $\Psi(r) \sim \exp(-A\sqrt{r_{\rm H}/r})$. Here, $r_{\rm out}$ is the outer disk radius and the constant A is of the order of unity. Assuming a Kepler law for the disk rotation and additionally that the foot points of the flux surfaces rotate with Kepler speed, a possible rotation law for the field lines can be derived. Inverting the above disk flux distribution then leads to the rotation law $\Omega_{\rm F}(\Psi) \sim |\ln(\Psi)|^3$.

As a consequence of differential rotation, the shape and position of the light surface would become *a priori* unknown quantities. Since these are singular surfaces and have to be considered numerically like boundaries, this would involve serious numerical complications. For this reason, for the time being, we consider $\Omega_{\rm F}(\Psi)$ = const. For the rotational velocity of the field, a fraction of the black hole rotation is assumed,

$$\Omega_{\rm F}(\Psi) = \Omega_{\rm F} = \epsilon\, \Omega_{\rm H}\,, \qquad \epsilon < 1 \tag{19}$$

For $a = 0.8, \epsilon = 0.4$, the position of the asymptotic light cylinder is at $R_{\rm L} = 10\, M$.

There is strong indication that the superluminal jets originate very close to a central black hole at distances of a few horizon radii. For galactic sources, the argument is that the jet speed is close to the escape velocity near the horizon (see Mirabel & Rodriguez 1995). Standard models for BL Lacertae objects also put the jet formation close to the central source (see Kollgaard (1994) and references therein).

Thus, for these highly relativistic jet sources, the assumption of a constant rotation of the flux surfaces may well be applied. A problem might exist for only mildly relativistic jet motion.

4. Results and discussion

We now present numerical solutions for the jet magnetosphere. The field distribution is calculated under the assumption of a small plasma loading, or in other words, in the force-free limit. Although the calculations are not entirely self-consistent, these are the first calculations of a collimated global jet magnetosphere in the context of Kerr metric.

Similar to the special relativistic, or even the Newtonian case, in a general relativistic treatment, the singularity of the stream equation at the Alfvén radius (or light surface) leads to a "kinky" structure of the magnetic field at this position, unless the regularity condition is properly satisfied.

In our previous work (Fendt 1994, Fendt et al. 1995) we investigated this problem for fast rotating, stellar magnetospheres. We found that a field matching could be achieved by adjusting both the shape of the jet boundary ($r_{\rm jet}, \theta_{\rm jet}$) and the poloidal current distribution (via the parameter b). This procedure may be interpreted as an adjustment of "magnetic pressure equilibrium" between the regions inside and outside the light cylinder.

In order to obtain smooth solutions at the outer light surface for the Kerr metric jet solutions presented here, we applied the same technique derived earlier (Fendt 1994, Fendt et al. 1995). Again, we emphasize that in the presented solutions the regularity condition at the outer LS determines the shape and the location of the jet boundary in the collimation region.

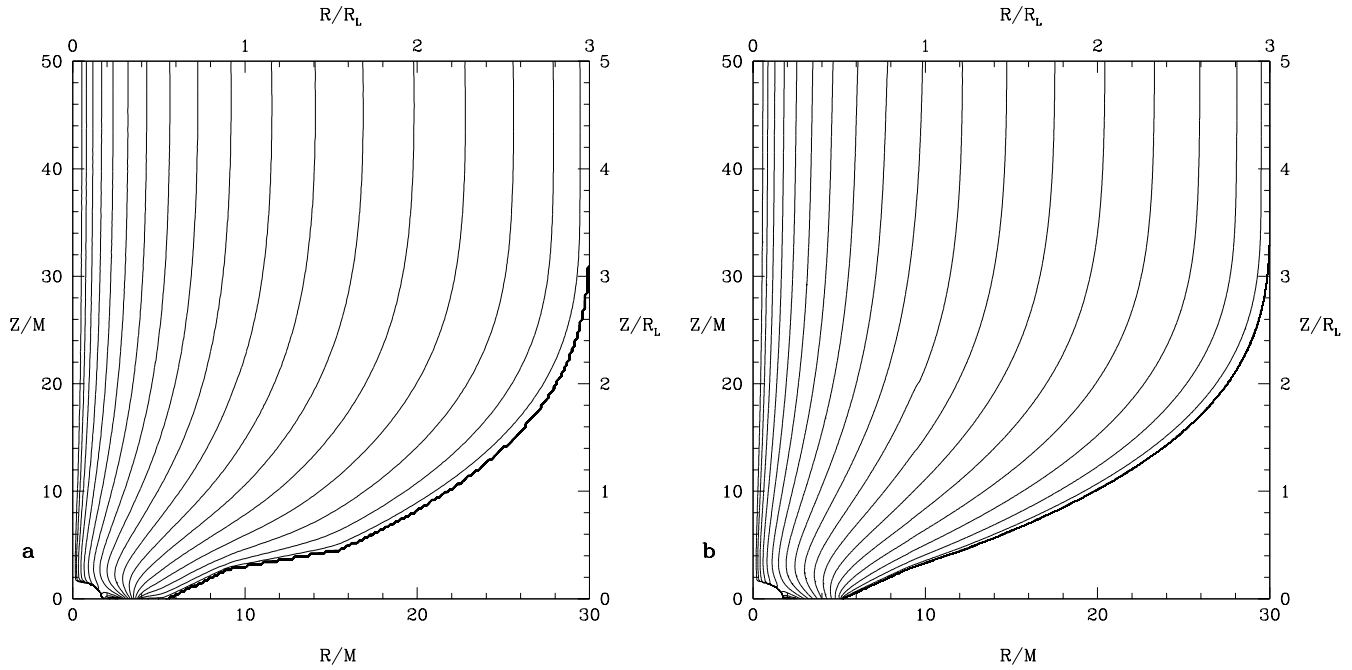

Fig. 2a and b. Magnetic flux surfaces Ψ of global Kerr jet solutions (a = 0.8, $(\Omega_{\rm F}/\Omega_{\rm H})$ = 0.4). The asymptotic jet radius is 3 asymptotic LC radii $R_{\rm L}$. Current distribution parameter **a** b = 1.0, g_I = 1.90, d = 2.29; **b** b = 0.8, g_I = 2.14, d = 2.71. Units: Ψ in $\Psi_{\rm max}$, contour levels 10^{-n^2}, n = 0, 1.8, 0.1; (R, Z) in $R_{\rm L}$ (upper and right axis), or in M (lower and left axis)

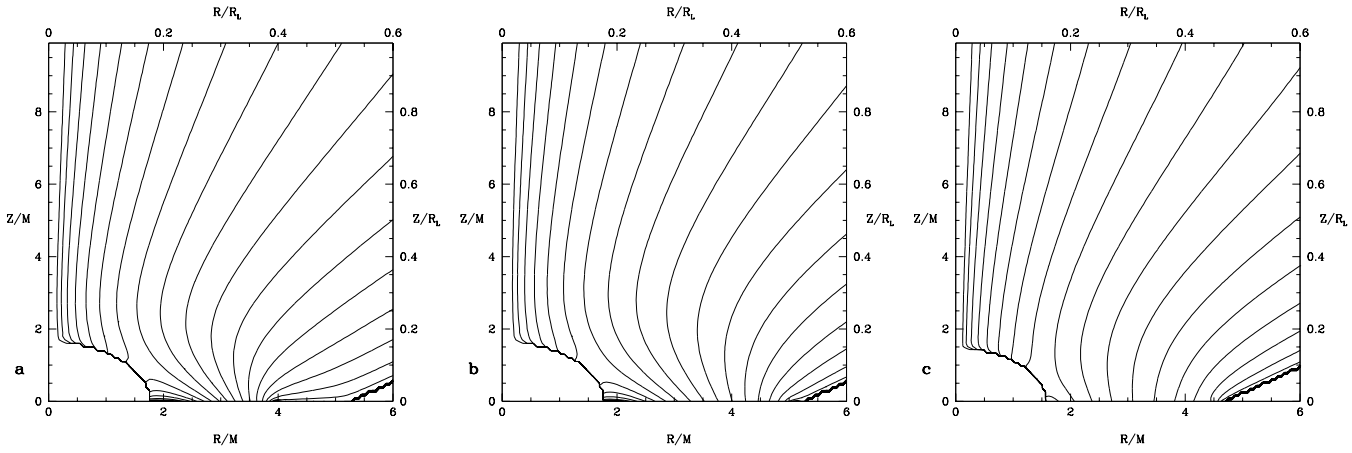

Fig. 3a–c. Magnetic flux surfaces of Kerr jet solutions. Subsets of the inner most regions with different choices of disk distribution. Disk flux distribution parameters **a** n = 4, r_o = 1.76, E = 0.05; **b** n = 3, r_o = 1.76, E = 0.03: **c** n = 2, r_o = 1.16, E = 0.05. The disk flux distribution is $\Psi_{\rm disk}(r, \pi/2) = E\,\Psi_{\rm max}(r - r_o)^n$ (see Appendix A.2). Units as in Fig. 2

4.1. The global jet solution

Fig. 2 shows two examples of global jet solutions extending from the inner LS to an asymptotic jet collimated to a cylindrical shape. The flux surfaces pass the outer LS smoothly.

The asymptotic jet radius is 3 $R_{\rm L}$ corresponding to 30 M for the parameters a = 0.8 and $(\Omega_{\rm F}/\Omega_{\rm H})$ = 0.4, or

$$R_{\rm jet} = \begin{cases} 1.5\,10^7 \ \left(M/5\,{\rm M}_\odot\right)\ {\rm cm} \\ 3.0\,10^{16}\ \left(M/10^{10}\,{\rm M}_\odot\right)\ {\rm cm}\,. \end{cases}$$

The asymptotic jet radius is basically parameterized in terms of the outer LS, i.e. in terms of the rotational velocity of the field. We chose $\Omega_{\rm F} = 0.4\Omega_{\rm H}$ under the assumption that the jet is launched within a distance of some $r_{\rm H}$ from the black hole.

If the field was rotating slower, when the flux surfaces originate further out in the disk, the asymptotic jet radius would be larger. With e.g. a = 0.8 and $(\Omega_{\rm F}/\Omega_{\rm H})$ = 0.1, we obtain an asymptotic jet radius 4 times larger. Note that the linear scaling in terms of $R_{\rm L}$ remains the same. It changes, however, in terms of $r_{\rm H}$.

We report that we were not able to obtain jet solutions with $R_{\rm jet} > 4R_{\rm L}$. The numerical procedure converges in the asymptotic region for asymptotic 1D solutions with any jet radius. However, it does not for a lower boundary condition, which is even slightly different from the asymptotic solution, and thus implying a field curvature. This negative result is not caused by numerical problems. It does not depend on numerical parameters like element size.

Instead, we take this as an indication for an upper limit for the jet radius,

$$R_{\rm jet} < 4\,R_{\rm L}\,, \tag{20}$$

of a cylindrically collimated, rigidly rotating, force-free magnetic jet.

On the other hand, differential rotation or plasma inertia may open up the jet structure. Both effects lead to an increase of poloidal current. The question is whether the corresponding de-collimating toroidal field pressure will supersede the effect by collimating tension. We suppose that the differential rotation plays a minor role as long as all the flux originates within a small region in the disk.

The jet solutions presented here are not 'self-collimated'. The prescription of an *asymptotic* jet boundary may be interpreted as an external pressure from the surrounding material. However, the shape of the collimating jet radius $R_{\rm jet}(Z)$ is determined by the regularity condition and/or the current distribution in the jet, and hence, is determined by the *internal* force-balance.

How the internal force-equilibrium affects the shape of the collimating jet can be seen in Fig. 2. In both solutions, the adjustment procedure (shape of jet boundary $\leftrightarrow$ distribution parameter b) was performed until the regularity condition is properly fulfilled. The two solutions have different poloidal current distributions, $I(\Psi)$. In comparison to the flux distribution with the broader current distribution (b = 0.8), the solution with the more concentrated current distribution (b = 1.0) involves an enhanced expansion (a slight de-collimation) beyond the outer light surface in order to obtain matching between the outer and inner solution.

4.2. The central domain and possible mass flow distribution

Fig. 3 shows subsets of the innermost part around the black hole from global solutions for different disk boundary conditions. These near-disk solutions might be interpreted as a disk corona. The overall picture could be summarized as follows.

- There is magnetic flux outgoing towards the jet.
- There is magnetic flux ingoing towards the black hole (which is hidden behind the inner LS).
- The flux surfaces near the jet axis are not directly connected with the accretion disk.
- Depending on the disk magnetic flux distribution, the curvature of the field lines close to the disk is rather different.

If for the following we imagine a possible mass flow associated with the flux surfaces, we find three different flow regimes within the field distribution – an accretion region, an outflow region, and a region empty of a plasma flow.

The ingoing flux tubes would allow for magnetic accretion from outer parts directly into the black hole. It is however questionable, whether the field strength will be so strong that plasma is accreted along field lines or whether, on the contrary, accretion will be dominated by gravitation and will thereby determine the field topology. This question cannot be answered with the present, force-free approach and depends on parameters like field strength, mass flux, or magnetization.

Under the assumption of a finite flux distribution originating very close to the black hole, the inward-outward bending flux surfaces provide evidence for a hollow jet structure. Although we have to investigate the wind equation along the flux surfaces in order to gain detailed knowledge about the plasma flow behaviour, we believe that the following thoughts and considerations might be reasonable.

First, the slope of the flux surfaces is too small to allow for a 'centrifugal' acceleration of the plasma. Blandford & Payne (1982) obtained a minimum angle enclosed by the disk and flux surface of 60° for the onset of plasma acceleration. Although this result was specifically calculated for a self-similar differentially rotating field structure and a cold wind, we believe that we can use it as an estimate for our case. It seems to be obvious that along a flux surface perpendicular to the disk, a wind driven by centrifugal instability is not possible.

If we therefore consider a hot plasma, the thermal pressure in a hot disk corona has to accelerate the plasma from the disk to heights of about 4 horizon radii above the disk. Here, the slope of the flux surfaces becomes eventually less than the critical value, allowing for 'centrifugal' acceleration. Such strong thermal pressures would require a very hot corona. However, our own experience as well as results published in the literature, show that the slow magnetosonic point of a wind flow is always located very close to the injection point. Thus, thermal pressure is unlikely to be a driving force up to high altitudes above the disk.

Secondly, from our work on the cold relativistic wind equation (Fendt & Camenzind 1996), we know that the stationary character of the flow is very sensitive on the curvature of the poloidal field in the case of a high plasma magnetization. In regions where the slope of the field line changes, it is very likely that no stationary solutions of the wind equation are possible, indicating that here shocks and instabilities may arise. These shock waves could eventually be observed in the asymptotic AGN jet as the helically moving knots seen with the VLBI radio observations (e.g. Zensus et al 1995).

Thirdly, the flux surfaces near the axis are not connected with the disk boundary but with the inner LS. Blandford & Znajek (1977) argued that all particles moving along field lines passing the inner LS must travel inwards. Along these field lines no mass outflow from the disk is possible. We found no solutions with flux surfaces extending from the disk boundary towards the jet axis.

Being aware of the crudeness of the the preceding considerations, we conclude that in the solutions presented here the

plasma will only flow within a thin layer of about $0.1\,R_{\rm jet}$ near the jet boundary, basically forming a hollow jet structure. The inner 90% of the jet cross-section will be empty of plasma flow from the disk. This picture is in good agreement with radio observations of AGN jets revealing moving knots along helical trajectories (Steffen et al. 1995, Zensus et al. 1995). It also fits within recent kinematic radiation models explaining the parsec scale motion of the jet knots by the lighthouse effect (Camenzind & Krockenberger 1992).

4.3. Angular momentum loss and Poynting flux from the black hole

The magnetosphere - poloidal current system is associated with an angular momentum flow and Poynting flux (or luminosity). The total Poynting flux in the jet $P \sim \int \Omega_{\rm F}(\Psi) I(\Psi) d\Psi$ can be calculated, using the known current distribution,

$$P = \frac{I_{\rm max}\Psi_{\rm max}}{R_{\rm L}} \left(\frac{1}{1-e^{-b}} - \frac{1}{b} \right) \tag{21}$$

(see Appl & Camenzind 1993), revealing a similar value for both field distributions in Fig. 2, $P = 0.6\,\left(I_{\rm max}\Psi_{\rm max}/R_{\rm L}\right)$.

The angular momentum loss (dJ_h/dt) from the black hole into the jet follows from the integration of the current distribution for all flux surfaces leaving the horizon to the asymptotic jet,

$$\frac{dJ_h}{dt} = -I_{\rm max}\Psi_{\rm max}\frac{1}{c}\oint I(\Psi)d\Psi\,, \tag{22}$$

and similarly for the Poynting flux (see Okamoto 1992). The outermost flux surface Ψ_h leaving the black hole (or the inner light surface) to the asymptotic jet could be estimated from Fig. 2 and Eq. (18). The integration gives

$$\frac{dJ_h}{dt} = -\frac{1}{c}\,I_{\rm max}\Psi_{\rm max}\left(\frac{\Psi_h + \frac{1}{b}\left(e^{-b\Psi_h}-1\right)}{1-e^{-b}} \right) \tag{23}$$

For the parameters of the solutions in Fig. 2, this gives an angular momentum loss from the black hole $(dJ_h/dt) \simeq 5.6\,10^{-14} I_{\rm max}\Psi_{\rm max}$ for the solution with a concentrated current distribution (Fig. 2a), and $(dJ_h/dt) \simeq 1.8\,10^{-14} I_{\rm max}\Psi_{\rm max}$ for the other one (Fig. 2b). Since the coupling g is similar for both solutions, their (dJ_h/dt) differ by a factor of 3.

What might be surprising with this result is that for two jet solutions with the same asymptotic jet radius, the same total magnetic flux and current flow, and also the same disk flux distribution, the angular momentum extraction from the black hole differs by a non-negligible value, which is determined by the *internal* structure of the jet magnetosphere. A similar calculation for the Poynting flux leads to $P_h \simeq 1.7\,10^{-3}(I_{\rm max}\Psi_{\rm max}/R_{\rm L})$ for the solution in Fig. 2a, and by the same factor 3 less for the other field distribution. The total angular momentum loss and Poynting flux in the jet differ only very few for both solutions.

We conclude this section with mentioning that the above estimates do not necessarely allow for an interpretation in terms of the dynamical evolution of the black hole. In our approach the flux surfaces emanating from the black hole/inner LS to the asymptotic jet also connect from the accretion disk to the black hole (with the same $I(\Psi)$). Thus, the same energy/angular momentum flow leaving the black hole also goes into the hole. What is important for the black hole evolution, are the total energy and angular momentum losses from the disk and the hole by the jet. However, the locally different structure of the current-magnetosphere system might affect the evolution of the accretion process and also radiative processes involved with the accretion.

5. Conclusion

In this work, we presented numerical solutions of the 2D force balance equation for strongly magnetized jets originating from the inner part of an accretion disk surrounding a black hole. The calculations were performed on the background of Kerr geometry.

The model topology underlying the calculations basically follows the standard model for AGN. The jet magnetosphere originates very close to the black hole from an accretion disk. In the solutions presented here, the field rotates rigidly with a fraction of the rotational velocity of the hole. The solutions are global solutions extending from the black hole's inner light surface to an asymptotic jet at a distance of 50 horizon radii.

The asymptotic jet is collimated to a cylindrical shape in agreement with the high degree of collimation observed for extragalactic jets. With the chosen parameters for the rotation, the asymptotic jet radius is 3 light cylinder radii or 30 horizon radii. For a black hole mass of $10^{10}\,{\rm M}_\odot$, this corresponds to a jet radius of $3.0\,10^{16}$cm. We found indications for an upper limit for the asymptotic jet radius for a force-free, cylindrical jet of about 4 light cylinder radii.

The solutions satisfy the regularity condition at the light surfaces and cross the outer light surface smoothly, i.e. without unphysical kinks in the field lines. The matching across this critical surface is achieved by a proper iterative adjustment of the current distribution and the shape of the jet boundary. It therefore determines the shape of the jet in the collimation region.

The field distribution near the disk (the 'corona') is directly influenced by the disk flux boundary condition. In general, the field solutions allow for mass in-fall towards the black hole as well as for mass outflow towards the asymptotic jet. There is strong evidence for a hollow jet structure, i.e. for a mass flow only in the outermost layers of the jet. In the asymptotic regime only the outermost 10% of the jet (in terms of radius) are likely to contain a mass flow.

The angular momentum flow and Poynting flux from the black hole into the jet could be estimated since the current distribution is known. For the field distributions investigated the solution with a concentrated jet current distribution gives angular momentum and energy losses from the hole a factor 3 higher than the other one. However, the total losses by the jet differ only slightly.

Acknowledgements. This work was supported by Swedish Natural Science Research Foundation (NFR). I thank M. Camenzind and M. Haehnelt for ideas the numerical calculations in this paper took advantage from and R. Khanna for helpful discussions. F. Quist is acknowledged for reading the manuscript. I am grateful to the referee, I. Okamoto, for clarifying comments, and especially for suggesting an estimate of the energy and angular momentum losses of the black hole from the current distribution.

Appendix A: numerical details

A.1. Finite element solver

The GSS equation is solved by means of the method of finite elements. The original code was introduced by Camenzind (1987) for relativistic astrophysical MHD applications. Haehnelt (1990) extended the procedure for Kerr metrics. The further evolution (however in special relativity) by Fendt (1994) and Fendt et al. (1995), now enables the code for an integration throughout the singular surface of the light cylinder and the calculation of smooth, global solutions. For the present investigation the latest version of the code (Fendt 1994) was re-arranged for the application in Kerr geometry.

In the finite element approach the integration region G is discretized in a set of isoparametric curvilinear 8-node elements of the serendipity class (Schwarz 1984). Within each element the flux function Ψ is expanded as

$$\Psi(r,\theta) = \sum_{i=1}^{8} \Psi_i^{(e)}\, N_i(\zeta,\eta). \tag{A1}$$

$\Psi_i^{(e)}$ denote the magnetic flux at the nodal point i of the element (e) and (ζ,η) are rectilinear coordinates on the normalized element.

For a solution, the stream equation is multiplied by a test function N (Galerkin ansatz) and integrated over the 2D plasma domain G applying Green's identity. We end up with the *weak form* of the GSS equation,

$$\int_G \frac{\alpha\, D}{\tilde{\omega}}\, \nabla N \cdot \nabla\Psi\, dA = \int_G J\, N\, dA + \int_{\partial G} \frac{\alpha\, D}{\tilde{\omega}}\, N \frac{\partial\Psi}{\partial n}\, ds, \tag{A2}$$

where n now denotes the unit vector perpendicular to the boundary ∂G, dA and ds the area and boundary elements, and J the source term of the R.H.S. of Eq. (12). With Eq. (A1) the integral equation corresponds to a matrix equation

$$\mathsf{A}(\Psi)\ \Psi = \boldsymbol{b}(\Psi), \tag{A3}$$

with the integrals on each grid element

$$A_{ij}^{(e)} = \int_{G_e} \frac{\alpha\, D}{\tilde{\omega}} \left(\Delta\partial_r N_i\ \partial_r N_j + \partial_\theta N_i\ \partial_\theta N_j \right) \frac{dr\, d\theta}{\sqrt{\Delta}}, \tag{A4}$$

and

$$b_i^{(e)} = \int_{G_e} N_i\, J^{(e)}\, \frac{\rho^2}{\sqrt{\Delta}}\, dr\, d\theta + \int_{\partial D} \frac{D}{\tilde{\omega}}\, N_i\, \partial_n\Psi\, ds \tag{A5}$$

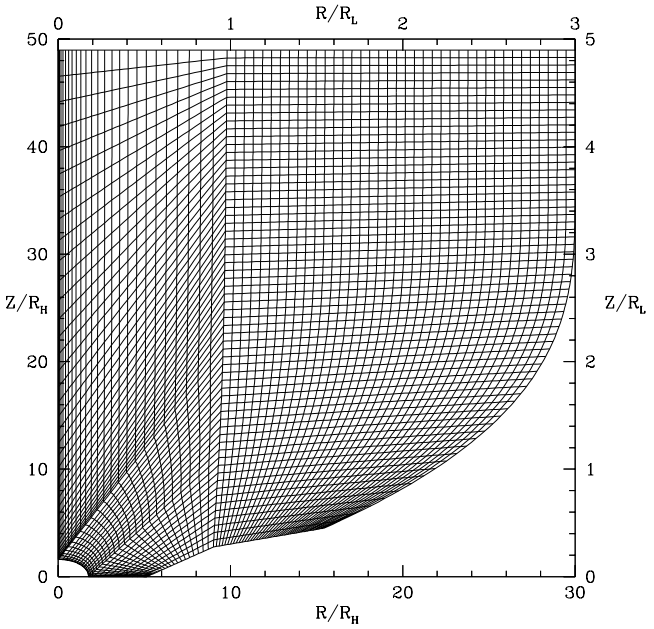

Fig. 4. Example of a numerical grid applied for the finite element code. The element boundaries must follow the shape of the two light surfaces

(Haehnelt 1990). Each component of Eq. (A3) corresponds to the force equilibrium between neighbouring nodal points of each element. Inversion of matrix equation (A3) eventually gives the solution $\Psi_i^{(e)}$ for each nodal point. The expansion (A1) provides the solution in any point $\Psi(r,\theta)$.

A.2. Boundary conditions

With the model assumptions discussed above, the computations have to satisfy the following boundary conditions.

- *Rotational axis*: $\Psi(r,0) = 0$.
- *Light surfaces*: Here, the regularity condition, Eq. (15), has to be satisfied. In the finite element approach this regularity condition is *automatically* satisfied. Like the homogeneous Neumann condition the regularity condition is a natural boundary condition on $D = 0$ in the sense that the surface integral (s. Eq. (A5)) does not contribute (see Fendt et al. 1995).
- *Disk surface*: Here, Ψ satisfies a Dirichlet condition, corresponding to a finite flux distribution,

  $$\Psi_{\rm disk}(r,\pi/2) = E\,\Psi_{\rm max}(r - r_o)^n\,. \tag{A6}$$

  For $r > (1/E)^{1/n} + r_o$, $\Psi_{\rm disk}(r,\pi/2) = 1$. The parameters r_o, E, n are chosen such that the foot points of the flux surfaces are concentrated to the innermost region. This is required by the assumption of a rigid rotation of the magnetosphere.
- *Jet boundary*: Along the jet boundary asymptotically collimating to a cylindrical shape we fix

  $$\Psi_{\rm max} = \Psi(r_{\rm jet},\theta_{\rm jet}) = 1 \tag{A7}$$

  by definition. As mentioned before, the shape of the jet boundary $(r_{\rm jet},\theta_{\rm jet})$ has to be well adjusted (and has to be

found in an iterative way) in order to satisfy the regularity requirement.

– *Asymptotic boundary* $(x, z_{\rm out})$: We assume that the jet has been collimated into a cylindrical shape. In this region with a distance of about $z \gtrsim 50\,{\rm M}$ from the black hole, the geometry is very close to Minkowski space. We use either homogeneous Neumann conditions or the non-linear analytic solution of the special relativistic, asymptotic jet equilibrium Eq. (17) as Dirichlet condition. When the outer and inner domain are calculated separately, then Dirichlet conditions are required at the upper boundary. Otherwise it would not be possible to fix the flux in this domain.

References

Abrahan, Z., et al., 1994, in J.A. Zensus, K.I. Kellermann (Eds), Compact Extragalactic Radio Sources, N.R.A.O., Socorro, p.87

Appl, S., Camenzind, M., 1993, A&A, 274, 699

Beskin, V.S., Pariev, V.I., 1993, Physics Uspekhi, 36, 529

Blandford, R.D., Znajek, R.L., 1977, MNRAS, 179, 433

Blandford, R.D., Payne, D.G., 1982, MNRAS, 199, 883

Blandford, R.D., 1990, in R.D. Blandford, H. Netzer, L. Woltjer, Active Galactic Nuclei, T.J-L. Courvoisier, M. Mayor (Eds), Lecture Notes, Saas-Fee Advanced Course 20, Springer, Heidelberg, p.242

Brandenburg, A., 1996, ApJ, 465, L115

Camenzind, M., 1986, A&A, 162, 32

Camenzind, M., 1987, A&A, 184, 341

Camenzind, M., 1990, Magnetized disk-winds and the origin of bipolar outflows, in: Klare, G. (Ed) Rev. Mod. Astron., 3, Springer, Heidelberg, p. 234

Camenzind, M., Krockenberger, M., 1992, A&A, 225, 59

Fendt, C., 1994, PhD thesis, University of Heidelberg

Fendt, C., Camenzind, M., Appl, S., 1995, A&A, 300, 791

Fendt, C., Camenzind, M., 1996, A&A, 313, 591

Ferreira, J., Pelletier, G., 1995, A&A, 295, 807

Haehnelt, M., 1990, Diploma thesis, University of Heidelberg

Khanna, R., Camenzind, M., 1992, A&A, 263, 401

Khanna, R., Camenzind, M., 1994, ApJ, 435, L129

Khanna, R., Camenzind, M., 1996a, A&A, 307, 665

Khanna, R., Camenzind, M., 1996b, in press

Kollgaard, R.I., 1994, Relativistic jets and the nature of BL Lacertae objects, in: Vistas in Astronomy, 38, 29

Macdonald, D., Thorne, K.,S., 1982, MNRAS, 198, 345

Macdonald, D., 1984, MNRAS, 211, 313

Michel, F.C., 1991, Theory of neutron star magnetospheres, The University of Chicago Press, Chicago

Mirabel, I.F., Rodriguez, L.F., 1994, Nature, 371, L46

Mirabel, I.F., Rodriguez, L.F., 1995, Superluminal motion in our Galaxy, in: H. Böhringer, G.E. Morfill, J.E. Trümper (Eds) 17th Texas Symposium on Relativistic Astrophysics and Cosmology, The New York Academy of Sciences, New York, p. 21

Okamoto, I., 1992, MNRAS, 254, 192

Sanders, D.B., Phinney, E.S., Neugebauer, G., Soifer, B.T., Matthews, K., 1989, ApJ, 347, 29

Scharlemann, E.T., Wagoner, R.V., 1973, ApJ, 182, 951

Schwarz, H.R., 1984, Methode der finiten Elemente, Teubner Studienbücher, Stuttgart

Steffen, W., Zensus, J.A., Krichbaum, T.P., Witzel, A., Qian, S.J., 1995, A&A, 302, 335

Thorne, K.S., Macdonald, D., 1982, MNRAS, 198, 339

Thorne, K.S., Price, R.H., Macdonald, D. (Eds), 1986, Black Holes: The membrane paradigm, Yale University Press, New Haven and London (TPM)

Tingay, S.J. et al., 1995, Nature, 374, 141

Takahashi, M., Nitta, S., Tatematsu, Y., Tomimatsu, A., 1990, ApJ, 363, 206

Thorne, K.S., Macdonald, D., 1982, MNRAS, 198, 339

Zensus, J.A., Cohen, M.H., Unwin, S.C., 1995, ApJ, 443, 35

Znajek, R.L., 1977, MNRAS, 179, 457

This article was processed by the author using Springer-Verlag LaTeX A&A style file *L-AA* version 3.